THE PUBLISHING HOUSE
OF THE ROMANIAN ACADEMY

PROCEEDINGS OF THE ROMANIAN ACADEMY, Series A,
Volume 24, Number 4/2023, pp. 373–381
DOI: 10.59277/PRA-SER.A.24.4.09

CONTRIBUTIONS TO THE DEVELOPMENT OF A NEW FAMILY OF HYBRID DC-DC CONVERTERS

Nicolae MUNTEAN [1,2], Octavian CORNEA[2], Dan HULEA[1,2], Mihăiță GIREADĂ[2], Dănuț VITAN [2]

[1] Romanian Academy, Timisoara Branch
[2] Politehnica University of Timișoara, Romania
Corresponding author: Nicolae MUNTEAN, E-mail: nicolae.muntean@ieee.org

Abstract. The paper presents a synthesis of the author contributions in developing a new class of DC-DC hybrid converters (HDC) with large voltage conversion ratio. The HDC structures are obtained by introducing commutated inductive and capacitive cells in the classical DC-DC converters. With these topologies, the voltage conversion ratio is larger, at the same duty cycle, compared with the classical converters. The paper presents some of the developed configurations, with unidirectional and bidirectional power flow, and some corresponding applications in renewable energy conversion and automotive industries.

Key words: DC-DC converter topology, bidirectional, wide ratio, switched capacitors, switched inductors.

1. INTRODUCTION

DC-DC converters (DC) are a class of power electronics equipment, which has shown a particularly positive dynamic in recent years, supported mainly by the renewable energy industries, DC power distribution, automotive, telecommunications, lighting, IT and aerospace [1–3].

Large voltage conversion ratio can be implemented with non-isolated structures, with multiple passive components [4, 5], hybrid switched capacitors [6, 7], switched inductors [8, 9], or a combination of switched capacitors and switched inductor structures[10–17].

The hybrid DC-DC converters, the main subject of this work, were developed starting from the papers published by B. Axelrod, Y. Berkovich, and A. Ioinovici [14], who proposed the integration in the classical DC-DC converters (Buck, Boost, Buck-Boost, Cůk, Sepic and Zeta) a commutated inductive or capacitive cells. In "step-down" converters, the cells structures are presented in Fig. 1. For "step-up" configurations the inductive and capacitive cells are presented in Fig. 2.

A synthetic overview of classical DC-DC converters, and the corresponding basic hybrid structures, using capacitive and inductive cells, is presented in Table 1, where V_{in}, V_{out} and D are the input, the output converters voltages, and the duty cycle respectively.

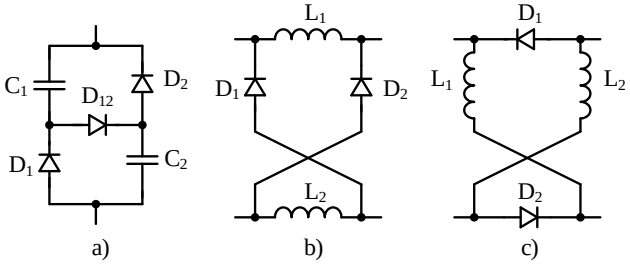

Fig. 1 – Capacitive and inductive cells used in "step-down" DC-DC converters: a) down 1; b) down 2; c) down 3.

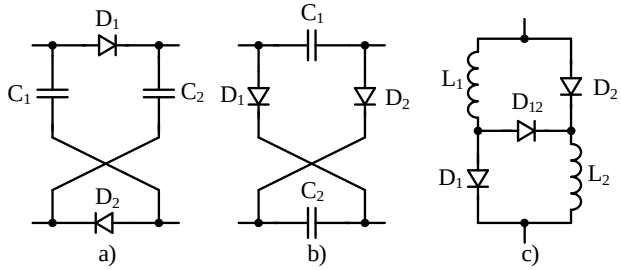

Fig. 2 – Capacitive and inductive cells used in "step-up" DC-DC converters: a) up 1; b) up 2; c) up 3.

Table 1

The V_{out} / V_{in} relation as a function of D

Cell Convertor	Gain	DOWN1	DOWN2	DOWN3	UP1	UP2	UP3
Buck	D	$\frac{D}{2-D}$	$\frac{D}{2-D}$				
Boost	$\frac{1}{1-D}$				$\frac{1+D}{1-D}$		$\frac{1+D}{1-D}$
Buck-Boost	$\left\lvert\frac{D}{(1-D)}\right\rvert$	$\frac{D}{(1-D)(2-D)}$			$\frac{2D}{1-D}$		$\frac{2D}{1-D}$
Cŭk	$\left\lvert\frac{D}{(1-D)}\right\rvert$	$\frac{D}{2(1-D)}$	$\frac{D}{2(1-D)}$			$\frac{1+D}{1-D}$	$\frac{D(1+D)}{1-D}$
Sepic	$\left\lvert\frac{D}{(1-D)}\right\rvert$	$\frac{D}{(1-D)(2-D)}$		$\frac{D}{2(1-D)}$			$\frac{D(1+D)}{1-D}$
Zeta	$\frac{D}{1-D}$		$\frac{D}{2(1-D)}$			$\frac{D}{2(1-D)}$	$\frac{D(1+D)}{1-D}$

In the next sections two of the developed hybrid converters will be presented with analytical description, experimental results and implemented applications: one, the first structure developed for a small power wind energy conversion system (WECS), and the last converter for an electric drive application in e-mobility. Both applications were developed in research programs, financed by an EEA grant and, respectively, by the Romanian Government.

From each configuration extended presentations can be found in the corresponding references published by the authors at international journals and conferences.

2. HYBRID BUCK SWITCHED-INDUCTOR DC-DC CONVERTER

The hybrid Buck switched-inductor DC-DC converter (SIHDC) is obtained by inserting an inductive cell (Down 2) in a Buck converter Fig. 3 [18]. The corresponding SIHIC circuit states for t_{on} (T_1 is ON) and t_{off} (T_1 is OFF, and D_1 and D_2 are ON) are presented in Fig. 4, where the switching period $T_S = t_{on} + t_{off}$. The main operation waveforms are presented in Fig. 5. The voltage ratio as a function of the duty cycle is given by:

$$\frac{V_{out}}{V_{in}} = \frac{D}{2-D}, \quad D = \frac{t_{on}}{T_S}. \tag{1}$$

The converter was designed in order to be implemented in a small power (5kW) WECS, presented in Fig. 6, where: PMSG is a permanent magnet synchronous generator, DB is a diode bridge, SC is a supercapacitor, CHRG represents the charger for a battery bank (BK), and INV is the inverter used for converting the DC voltage in AC single phase voltage.

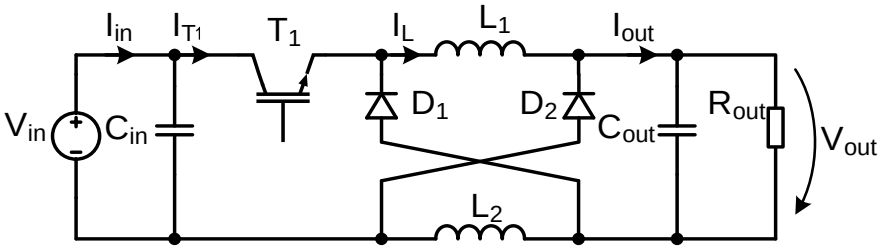

Fig. 3 – The hybrid Buck switched-inductor DC-DC converter.

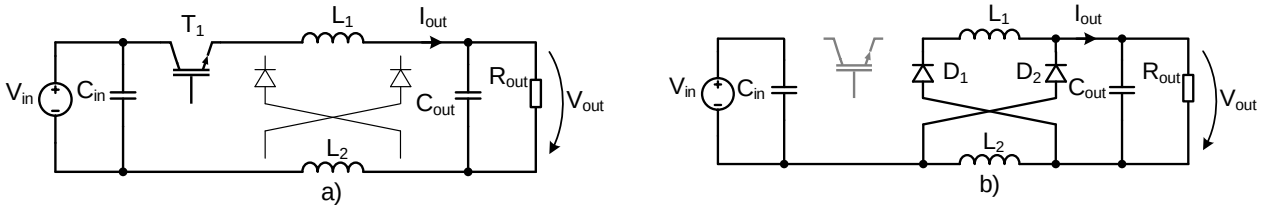

Fig. 4 – Converter circuit states for: a) t_{on}; b) t_{off}.

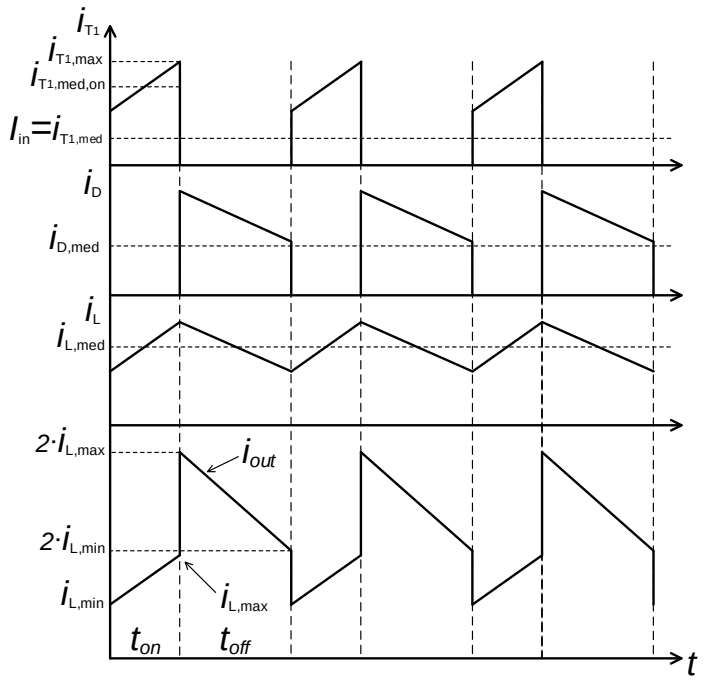

Fig. 5 – Theoretical waveforms of the Improved SIHDC converter.

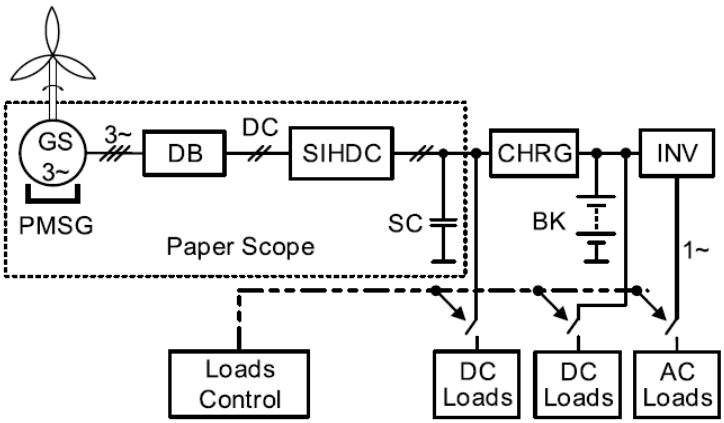

Fig. 6 – The WECS configuration and components.

The SC acts a primary energy storage element, necessary to have a high-power density, in order to be capable of extracting and storing the maximum power from the generator. The WECS control uses a classical MPPT algorithm. The SIHDC implements a current control, designed after a complete stability analysis [18]. Some experimental results for the convertor currents are given in Fig. 7. The SIHDC specifications are given in Table 2. Experimental results, obtained in the field, in the WECS testing procedures, were presented in Fig. 8. The SIHDC prototype and the wind turbine images are presented in Fig. 9.

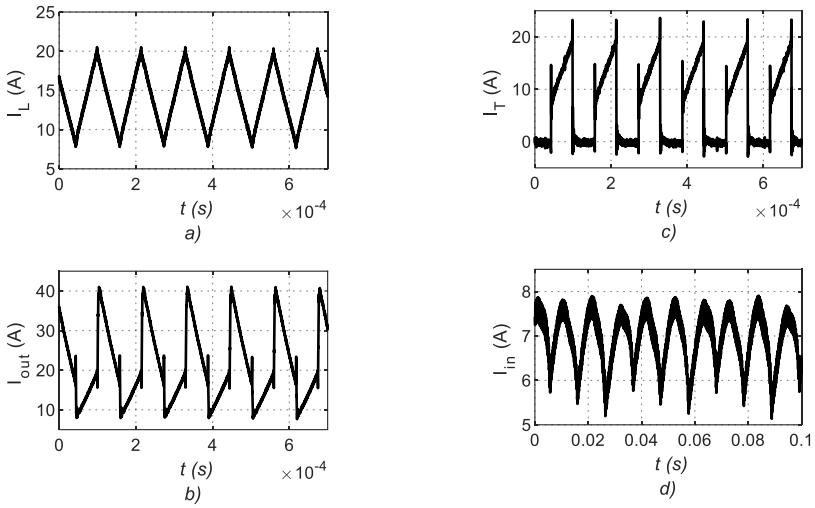

Fig. 7 – a) The L_1 (L_2) current; b) the output current; c) the transistor current; d) the input current

Table 2

SIHDC Specifications

Symbol	Value	
P_{max}	5	kW
V_{in}	130–400	V
V_{out}	50–120	V
f_s	9	kHz
$L_1 = L_2 = L$	170	µH
$r_{L1} = r_{L2} = r_L$	6	mΩ
C_{in}	10	mF
C_{out}	12	mF
SC	63	F

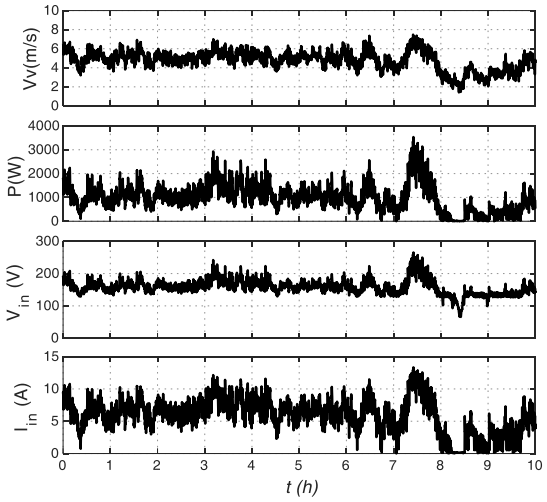

Fig. 8 – Input power (P_{in}), input voltage (V_{in}), and current (I_{in}) as a function of wind speed (V_v)

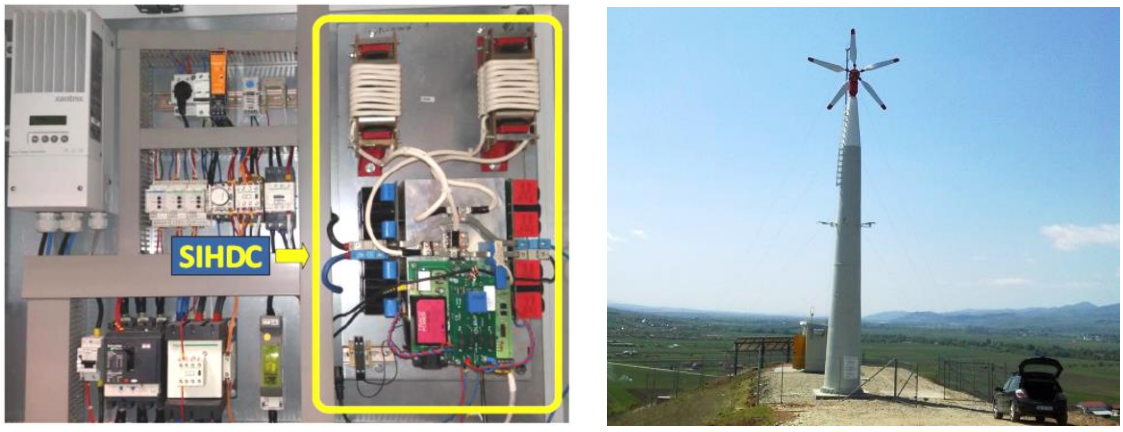

Fig. 9 – SIHDC prototype and the wind turbine images.

3. IMPROVED BIDIRECTIONAL HYBRID SWITCHED CAPACITOR CONVERTER (BHSC)

The BHSC [14, 20], shown in Fig. 10 is derived from the unidirectional hybrid converter with switched capacitors, originally proposed in several papers [1, 14], as a boost converter. This converter resembles a conventional boost converter with a capacitive switching cell, connected to the output.

In unidirectional mode, the capacitors are charged in parallel and discharged in series, thus obtaining a doubling effect of the output voltage. For BHSC converter operating in buck mode, an additional halving of the voltage is obtained. Elimination of high frequency voltages between the two inputs is achieved with each inductor at the two inputs being split. These two inductors can be designed as separate inductors, if commercially available inductors are desired, or they can be magnetically coupled, when there is a need for a compact design. This new topology of the improved BHSC is shown in Fig. 11.

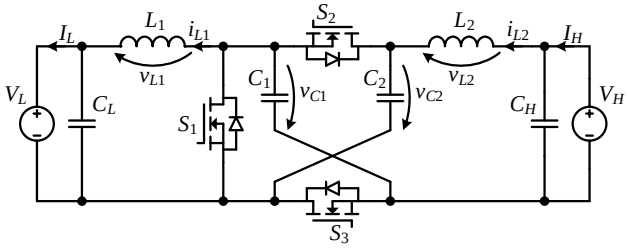

Fig. 10 – BHSC.

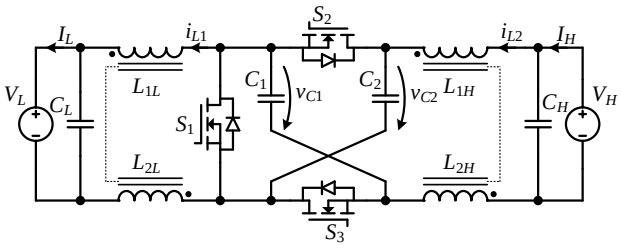

Fig. 11 – Improved BHSC.

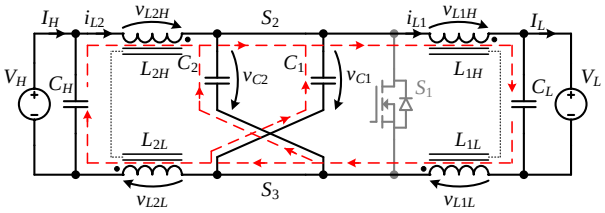

Fig. 12 – Improved BHSC equivalent circuit for t_{on} (S_2, S_3 – ON, S_1 – OFF).

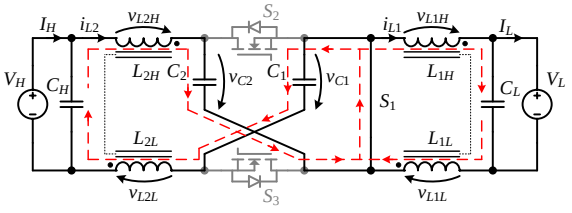

Fig. 13 – Improved BHSC equivalent circuit for t_{off} (S_2, S_3 – OFF, S_1 – ON).

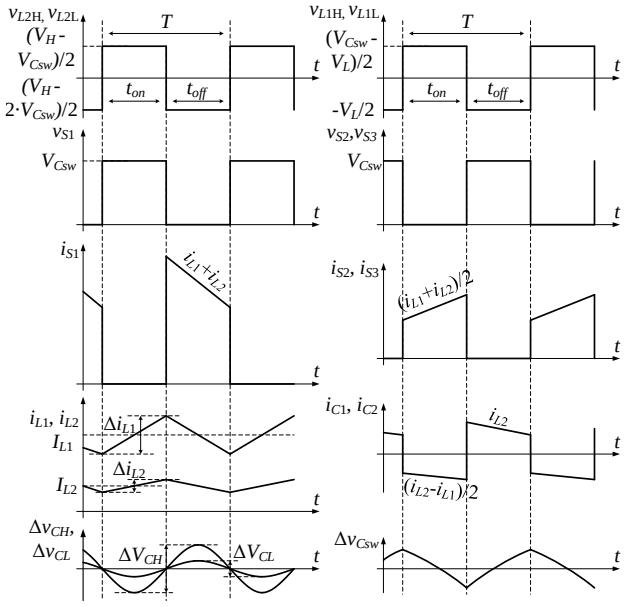

Fig. 14 – Theoretical waveforms of the Improved BHSC converter.

The improved BHSC operates in a comparable way to the conventional BHSC converter if each split inductor is viewed as one. The two equivalent switching schematics for the t_{on} and t_{off} intervals, are presented in Fig. 12 and Fig. 13. During t_{on}, the two switched capacitors (C1 and C2) are connected in parallel. In buck

mode the switched capacitors are discharged to V_L and charging with a smaller current from V_H, and vice versa for boost mode. During t_{off} , the two switched capacitors are connected in series. In buck mode the switched capacitors are charged from V_H and, in boost mode they are discharged to V_H. The main operation waveforms are presented in Fig. 14. Considering the duty cycle, D, defined for the t_{on} , the ratio between the two input voltages is calculated in steady state, as following:

$$V_L = V_H \cdot \frac{D}{2-D}. \tag{2}$$

The project goal was the development of a reduced scale (reduced power) laboratory demonstration model for an urban electric transportation energy conversion system, using supercapacitors (SC) as main energy storage devices and a super-high torque/power density interior permanent magnet synchronous motor/drive [21]. The block diagram of the studied concept is presented in Fig. 15.

The energy conversion and storage system (ECSS) are composed of: bidirectional DC-DC converter-supercapacitor units (CSU), backup battery module (BM) and electric drive (ED). ECSS operating modes are charging, driving and regenerative braking.

In charging mode, ECSS is connected to the charging station. The supercapacitors are charged fast, at the maximum allowed current, controlled by the bidirectional DC-DC converters (BHDC). In driving mode, ECSS is disconnected from the charging station, therefore energy being taken from SCs through BHDC and delivered to the ED. During the regenerative braking periods, the energy is taken from ED through the bidirectional DC-AC converter and transferred to the DC voltage bus. Depending on the level of DC voltage bus the BHDC uses this energy to charge the SCs at constant current.

The main idea in the implementation was the use of half bridge modules. By using half bridge modules, the manufacturing process of the converter is improved, and the parasitic inductances are reduced in the switching loops. GaN switching devices were used in order to achieve better efficiency [22]. The Half Bridge modules are presented in Fig. 16, the improved BHSC can be observed in Fig. 17.

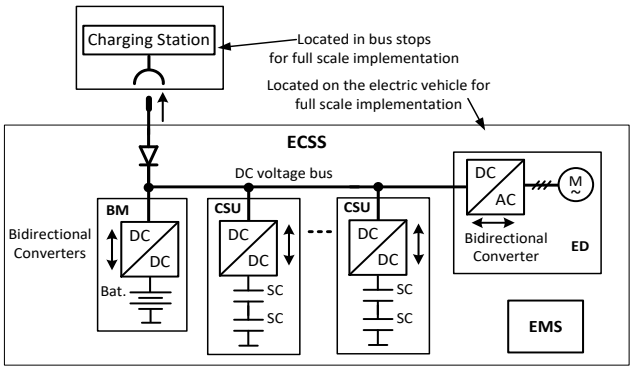

Fig. 15 – Block diagram of the proposed demonstration model.

Fig. 16 – GaN Half Bridge.

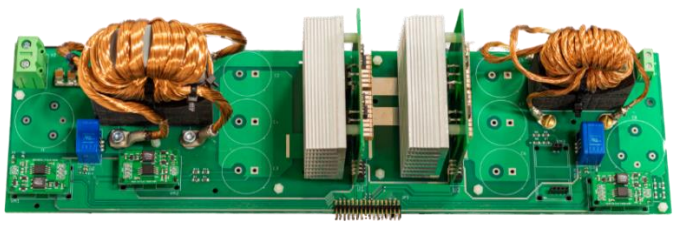

Fig. 17 – Improved BHSC.

Prototype parameters for I-BHSC are presented in Table 3. Experimental results for $V_H = 375$V, $V_L = 80$V, and $I_{L1} = 22$A, are presented in Figs. 18–19 for the main waveforms, and in Fig. 20 for the capacitor ripples. Using a PI regulator to control I_{L1} current, the transition between buck to boost and reverse is achieved and shown in Fig. 21.

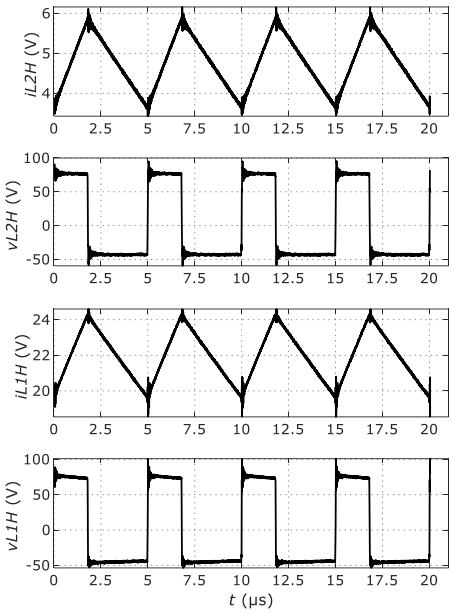

Fig. 18 – Inductor current and voltage waveforms.

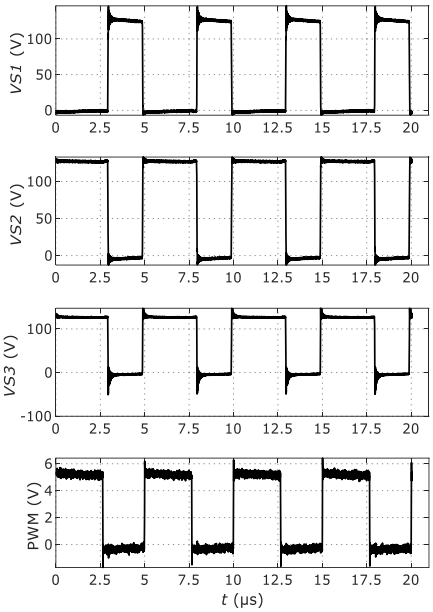

Fig. 19 – Transistor voltages, and PWM signal.

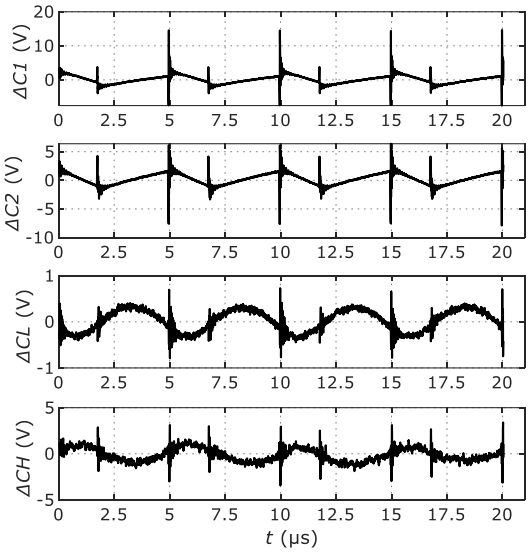

Fig. 20 – Capacitor voltage ripple waveforms.

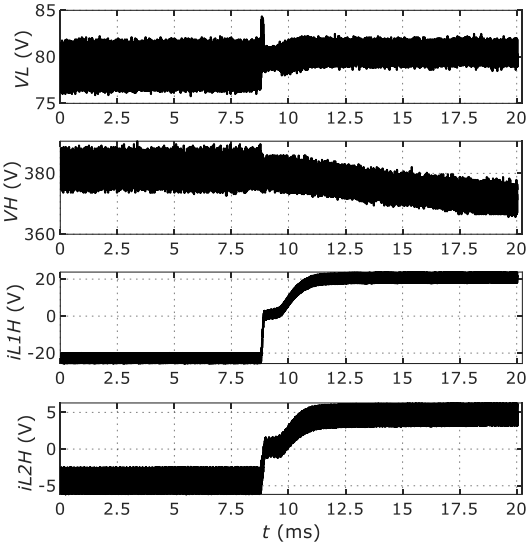

Fig. 21 – Boost to Buck transition.

Table 3

BHSC prototype parameters

Element	Value	Unit	Description
V_H	400	V	High voltage input maximum value
V_L	0–160	V	Low voltage input maximum value
I_H	17.5	A	High voltage input maximum current
I_L	43.75	A	Low voltage input maximum current
f	200	kHz	Switching frequency
L_1	39	μH	Design value inductance
L_2	98	μH	Design value inductance
C_1, C_2	20	μF	Switched capacitors 2
C_H	500	nF	High voltage input capacitance
C_L	3.4	μF	Low voltage input capacitance

4. CONCLUSIONS

Large voltage conversion ratio in DC-DC converters is a requirement in a lot of applications in automotive industry and renewable energy conversion systems. Classical non-isolated DC-DC converters can be easily transformed into hybrid converters using inductive and/or capacitive commutated cells.

Bidirectional power flow can also be obtained.

SC represents a storage technology, in continuous development, with relatively high-power density compared with batteries.

The energy stored in SC depends on the voltage levels across its terminals, which change within wide limits, when it is charged or discharged. This is one of the reasons why it is necessary to use a dedicated DC-DC converter with high voltage conversion ratio, in systems with SC.

Both applications, described in the previous chapters, use SC for energy storage.

In the first energy conversion system a unidirectional HDC, as an interface between the PMSG and the SC, was implemented. It was obtained including an inductive cell in a classical Buck DC-DC converter and ensures the fast charging of SC in a small power WECS.

The second application implements a bidirectional power flow HDC, with capacitive cell, also as interface between SC, the drive and the charging station, in an automotive application.

Both converters were studied theoretically, and were tested in laboratory prototypes.

The results prove that the proposed hybrid DC-DC structures are a proper candidate in applications with large voltage conversion ratio.

REFERENCES

1. N. CLARK, E. MOTTO, S. SHIBATA, *New SLIM Package Intelligent Power Modules (SLIMDIP) with thin RC-IGBT for consumer goods applications*, 2015 IEEE Energy Conversion Congress and Exposition (ECCE), Montreal, QC, Canada; IEEE, Sep. 2015, pp. 4510–4512, DOI: 10.1109/ECCE.2015.7310296.
2. J.M. MAZA-ORTEGA, E. ACHA, S. GARCÍA, A. GÓMEZ-EXPÓSITO, *Overview of power electronics technology and applications in power generation transmission and distribution*, J. Mod. Power Syst. Clean Energy, **5**, *4*, pp. 499–514, 2017, DOI: 10.1007/s40565-017-0308-x.
3. Z. TANG, Y. YANG, F. BLAABJERG, *Power electronics: The enabling technology for renewable energy integration*, CSEE J. Power Energy Syst., **8**, *1*, pp. 39–52, 2021, DOI: 10.17775/CSEEJPES.2021.02850.
4. V. MARZANG, S.H. HOSSEINI, N. ROSTAMI, P. ALAVI, P. MOHSENI, S.M. HASHEMZADEH, *A high step-up nonisolated DC-DC converter with flexible voltage gain*, IEEE Trans. Power Electron., **35**, *10*, pp. 10489–10500, 2020, DOI: 10.1109/TPEL.2020.2976829.
5. S. MISAL, M. VEERACHARY, *Analysis of a fourth-order step-down converter*, IEEE Trans. Ind. Appl., **56**, *3*, pp. 2773–2787, 2020, DOI: 10.1109/TIA.2020.2975500.
6. O. CORNEA, G.-D. ANDREESCU, N. MUNTEAN, D. HULEA, *Bidirectional power flow control in a DC microgrid through a switched-capacitor cell hybrid DC-DC converter*, IEEE Trans. Ind. Electron., **64**, *4*, pp. 3012–3022, 2017, DOI: 10.1109/TIE.2016.2631527.
7. Y. ZHANG, J. LIU, X. MA, *Using RC type damping to eliminate right-half-plane zeros in high step-up DC-DC converter with diode capacitor network*, 2013 IEEE ECCE Asia Downunder, Jun. 2013, pp. 59–65, DOI: 10.1109/ECCE-Asia.2013.6579074.
8. Y. TANG, T. WANG, *Study of an improved dual-switch converter with passive lossless clamping*, IEEE Trans. Ind. Electron., **62**, *2*, pp. 972–981, Feb. 2015, DOI: 10.1109/TIE.2014.2341608.
9. G.G. KUMAR, K. SUNDARAMOORTHY, V. KARTHIKEYAN, E. BABAEI, *Switched capacitor-inductor network based ultra-gain DC-DC converter using single switch*, IEEE Trans. Ind. Electron., **67**, *12*, pp. 10274–10283, 2020, DOI: 10.1109/TIE.2019.2962406.
10. P. CHAVOSHIPOUR HERIS, Z. SAADATIZADEH, M. SABAHI, E. BABAEI, *A new switched-capacitor/ switched-inductor-based converter with high voltage gain and low voltage stress on switches*, Int. J. Circuit Theory Appl., **47**, *4*, pp. 591–611, 2019, DOI: 10.1002/cta.2606.
11. D. HULEA, N. MUNTEAN, M. GIREADA, O. CORNEA, E. SERBAN, *Bidirectional hybrid switched-inductor switched-capacitor converter topology with high voltage gain*, EPE ’19 ECCE Europe, Genova, Italy, 2019, DOI: 10.23919/EPE.2019.8915535.
12. M.A. SALVADOR, T.B. LAZZARIN, R.F. COELHO, *High step-up DC–DC converter with active switched-inductor and passive switched-capacitor networks*, IEEE Trans. Ind. Electron., **65**, *7*, pp. 5644–5654, 2018, DOI: 10.1109/TIE.2017.2782239.
13. Z. SAADATIZADEH, P.C. HERIS, Y. YANG, F. BLAABJERG, *High step-up/down switched-capacitor based bidirectional DC-DC converter*, 2020 IEEE 21st Workshop on Control and Modeling for Power Electronics (COMPEL), Aalborg, Denmark, Nov. 2020, DOI: 10.1109/COMPEL49091.2020.9265735.

14. B. AXELROD, Y. BERKOVICH, A. IOINOVICI, *Switched-capacitor/switched-inductor structures for getting transformerless hybrid DC–DC PWM converters*, IEEE Transactions on Circuits and Systems, **55**, *2*, pp. 687–696, 2008.
15. N. TEWARI, V.T. SREEDEVI, *Switched inductor-switched capacitor based high gain hybrid DC-DC converter*, 2018 8th IEEE India International Conference on Power Electronics (IICPE), Jaipur, India, Dec. 2018, DOI: 10.1109/IICPE.2018.8709537.
16. M.S. BHASKAR, V.K. RAMACHANDARAMURTHY, S. PADMANABAN, F. BLAABJERG, D.M. IONEL, M. MITOLO, D. ALMAKHLES, *Survey of DC-DC non-isolated topologies for unidirectional power flow in fuel cell vehicles*, IEEE Access, **8**, pp. 178130–178166, 2020, DOI: 10.1109/ACCESS.2020.3027041.
17. A. ANDRADE, T. FAISTEL, R. GUISSO, A. TOEBE, *Hybrid high voltage gain transformerless DC-DC converter*, IEEE Trans. Ind. Electron., **69**, *3*, pp. 2470–2479, 2022, DOI: 10.1109/TIE.2021.3066939.
18. O. CORNEA, D. HULEA, N. MUNTEAN, G.-D. ANDREESCU, *Step-down switched-inductor hybrid DC-DC converter for small power wind energy conversion systems with hybrid storage*, IEEE Access, **8**, pp. 136092–136107, 2020, DOI: 10.1109/ACCESS.2020.3012029.
19. H. NOMURA, K. FUJIWARA, M. YOSHIDA, *A new DC-DC converter circuit with larger step-up/down ratio*, 37th IEEE Power Electronics Specialists Conference, Jeju, Korea, 2006, DOI: 10.1109/PESC.2006.1712228.
20. D. HULEA, M. GIREADĂ, O. CORNEA, N. MUNTEAN, *An improved bidirectional hybrid switched capacitor converter*, IECON 2022, Brussels, Belgium, 2022, DOI: 10.1109/IECON49645.2022.9969058.
21. L.-D. VITAN, A. MARTIN, L. TUTELEA, I. BOLDEA, I. TORAC, N. MUNTEAN, *Supercapacitor city minibus bonded – NdFeB IPMSM propulsion system: design and system modeling methodology via a case study and laboratory experiments*, IEEE Transactions on Industry Applications, **59**, *2*, pp. 1405–1417, 2023, DOI: 10.1109/TIA.2022.3220500.
22. D. HULEA, B. FAHIMI, N. MUNTEAN, O. CORNEA, *High ratio bidirectional hybrid switched inductor converter using wide bandgap transistors*, 20th European Conference on Power Electronics and Applications (EPE'18 ECCE Europe), 2018.

Received June 20, 2023